

# 3D RECONSTRUCTION OF ROADS AND TREES FOR CITY MODELLING

George Vosselman

Department of Geodesy, Delft University of Technology, Thijsseweg 11, NL-2629 JA Delft, The Netherlands  
g.vosselman@geo.tudelft.nl

Commission III, WG III/3

**KEY WORDS:** Laser altimetry, city modelling, cadastral maps, data fusion, 3D reconstruction.

## ABSTRACT:

Laser altimetry is a valuable data source for the production of 3D city models. For applications of 3D city models that are to provide a realistic impression of the urban environment, modelling of the buildings only is insufficient. This paper presents methods for the reconstruction of the street surfaces by combining airborne laser data with 2D information from a cadastral map. Locations of trees are also extracted from the laser data. With modelled street surfaces, trees and water surfaces added to reconstructed buildings a more realistic looking city model can be obtained.

## 1. INTRODUCTION

Most research projects on 3D reconstruction of city models from airborne laser altimetry data have been focussing on the reconstruction of buildings (Haala *et al.* 1998, Vosselman 1999, Routensteiner and Briese 2002). For a city model that is to be used for e.g. city planning and tourist guidance, a complete modelling of the urban environment is needed. For these city models 3D reconstruction of roads and trees is also required as these objects have a large impact on how a city is perceived.

This paper describes several algorithms and procedures developed for the 3D reconstruction of streets and trees from airborne laser altimetry data in combination with a cadastral map. This cadastral map is used to obtain the boundaries of the streets. The purpose of the street surface reconstruction is to smooth the laser data and to determine the heights of the street boundaries as extracted from the cadastral map in such a way that a realistic street surface is obtained (section 2). For the trees, the focus is on the automatic extraction of the tree locations from the laser data (section 3). The different processing steps are illustrated using data from the old downtown area of Delft. In order to complete a 3D city model, the buildings and canals in this area are modelled by flat surfaces inside the parcel boundaries extracted from the cadastral map (section 4).

## 2. MODELLING ROADS

Before the map and laser data can be combined in the estimation of the road surfaces, both data sources required several pre-processing steps. The original data sources and the pre-processing are discussed in the next two paragraphs. The strategies for the data fusion are described and analysed in the last paragraph of this section.

### 2.1 Preparation of the cadastral map

The obtained digital cadastral map consisted of all parcel boundaries. Whereas the street patterns are clearly recognisable from the parcel structures, the street parcels were not explicitly labelled. Labels of street parcels and canal parcels were added by hand (figure 1).

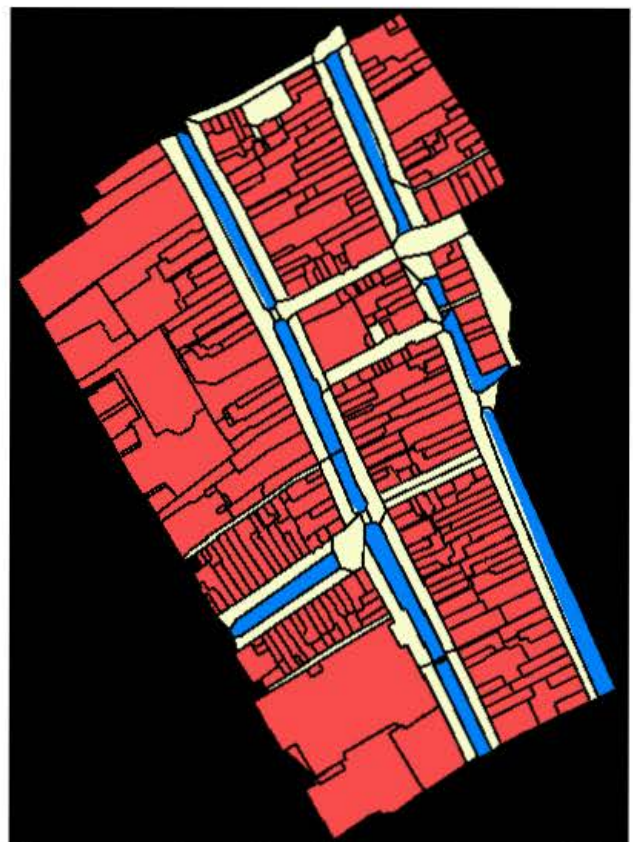


Figure 1: Edited part of the cadastral map with parcels labelled as building, road or canal.

Furthermore, some bridges over canals appeared to be missing in the parcel structure. From a cadastral point of view this may be of less interest, since both the bridges and the canals have the same owner. For the reconstruction of the city model, the bridges, however, are essential objects. Polygons outlining the bridges were manually added to the cadastral data.

In the last step of the map pre-processing, the points were inserted into the edges of polygons outlining the street parcels. Edges that are straight in 2D map, of course, do not need to be straight in 3D. To correctly capture the shape of the road surface, the edges therefore need to be described by more points. For this purpose, points were inserted into the edges of the street parcels at every 0.5 m. For all these points and the original map points the height needs to be determined from the laser data.

## 2.2 Selection of the laser data on the road surfaces

The laser data has been acquired with the TopoSys I scanner, flown at a height of about 1000 m. This resulted in a dense dataset with 10 cm and 2 m point spacing in flight direction and in scan line direction respectively (Baltasvias, 1999). With an opening angle of only 14 degrees, this scanner only results in small, occluded, areas in urban environments. The footprint size was about 0.5 m and last pulse data was recorded.

The laser points that are located within the street parcels have been selected in two steps. First a mask image was produced indicating whether pixels (partially) fall inside a street parcel or not. Laser points were initially selected with this mask image. For each of these selected points it was then checked whether a point was located inside the bounds of a street parcel. By this two step selection procedure, the number of computationally expensive inside-polygon-tests was drastically reduced.

Although within the street parcels, the selected points do not always correspond to pulse reflections on the street. Many pulses are reflected by objects like trees, cars, light poles and sunshades attached to buildings. Due to small inaccuracies in both the map and the laser point positions, reflections are also obtained from points of buildings and the water in the canals adjacent to the streets. For the estimation of the street surface, these points need to be filtered away. For the object points above the street level, a simple morphological filter based on maximum expected slopes in the terrain (Vosselman, 2000) is sufficient. Points reflected from the water surface, however, are below the street level and would lead to filtering away part of the points on the street. To correctly filter the points below the street level, it is better to first perform a segmentation of the point cloud based on local height difference and/or slopes. The large segments will correspond to the street level. By comparing the height of a DEM made of the large segments with the heights of points in small segments, some small segments may also be classified as terrain objects (Sithole and Vosselman, 2003).

Finally, the dataset was reduced in size by selecting only one point within a radius of 0.5 m. In this way the point spacing in scan line direction is maintained (at 2.0 m), but in flight direction about every 5<sup>th</sup> point is selected. With a footprint size of 0.5 m, the selected points no longer have overlapping footprints and enable a faster rendering of the produced 3D city model.

## 2.3 Estimation of the road surface

To create a data structure for determining neighbourhood relationships, a Delaunay triangulation was performed with the combined set of laser points and set of dense map points. To avoid interpolation across non-street areas, the boundaries of the street parcels were used to constrain the triangulation (figure 2).

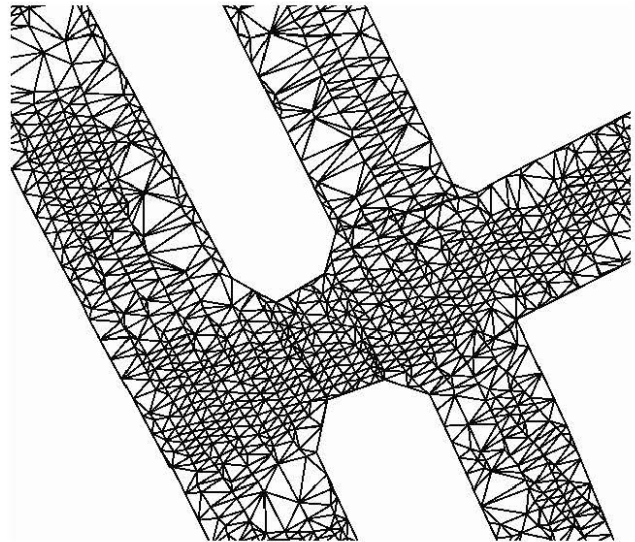


Figure 2: Constrained triangulation of the combined map and laser points within the streets objects. The varying point densities are due to occlusion of the street level by trees, cars and buildings.

A first estimation of the road surface was obtained by assigning to each map point the height of the nearest laser point. This results into the surface model shown in figure 3. Because of the small point distances already a little noise in the height data causes a large variation of the directions of the surface normals of the TIN faces. Rendering these faces results in a noisy appearance of the road surface.

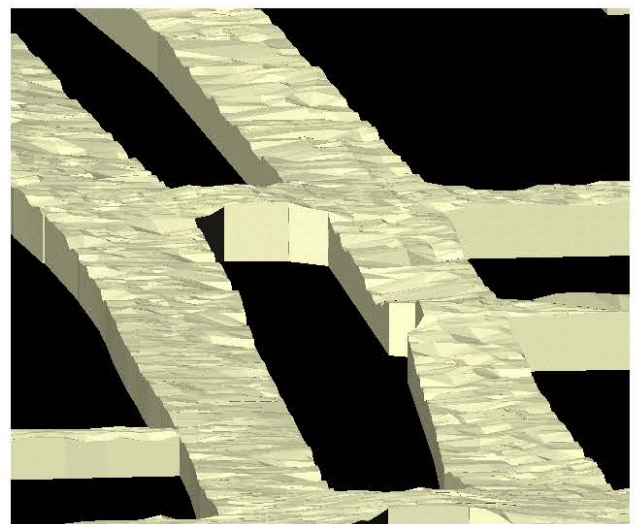


Figure 3: Original laser points combined with map points. The heights of the map points are inferred from the nearest laser points.

To obtain a more realistic view the height data has been smoothed by fitting 2<sup>nd</sup> order polynomial functions. 2<sup>nd</sup> order

polynomials were used to correctly model the relatively strong road curvature of the bridges across the canals. For each location of a laser point or a map point, the heights of all laser points within some radius were used for this estimation. Figure 4 shows that the noisy character of the laser points is strongly reduced by this smoothing. However, it also shows that the height near the roadsides is less smooth than near the road centrelines. These errors are caused by extrapolations of the 2<sup>nd</sup> order polynomials. Their coefficients are estimated with the heights of the laser points. However, when estimating the height at a map point location, all laser points are located on one side of this map point. In particular when the nearest laser points are a bit further away (due to occlusions of nearby street locations), the noise in the estimated coefficients will result in a very noisy height estimation of the map points.

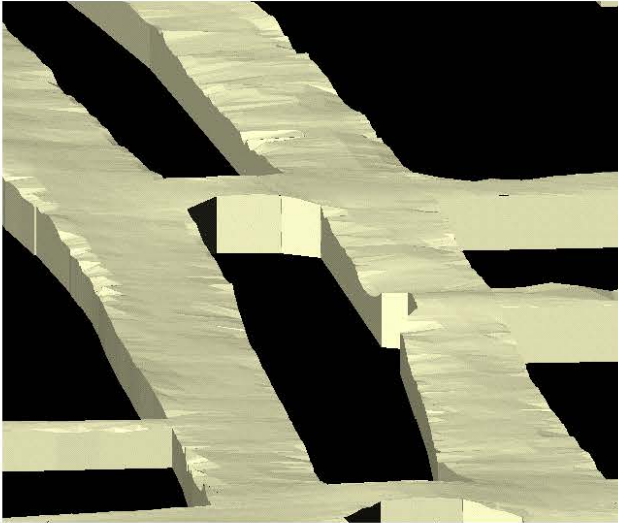


Figure 4: Road surface estimated by 2<sup>nd</sup> order polynomial fitting to near laser points.

For a correct extrapolation, the accuracy of the estimated coefficients is not high enough. In order to improve this we made use of the knowledge that the road curvature and road slope in across road direction can be neglected on straight road parts. Near road crossings, however, curvatures in the road surface do exist and should be estimated in the surface fitting.

Therefore, we first need to determine which points are located on straight road segments. For this purpose the cadastral map has been used. As described in paragraph 2.1 the map polygons exist of many short straight edges. A point can be classified as a point on a straight road segment if the nearby map edges exhibit a dominant direction. More formally, this is evaluated using the ratio of eigenvalues of a matrix with moments of the weighted edge direction vector components.

Let a map edge  $m$  be defined by the point pair  $(b, e)$  and let the map edge vector  $\vec{m}$  be expressed by its length multiplied by a direction vector  $\vec{n}$ :

$$\vec{m} = \begin{pmatrix} x_e - x_b \\ y_e - y_b \end{pmatrix} = \|\vec{m}\| \vec{n} = \|\vec{m}\| \begin{pmatrix} x_n \\ y_n \end{pmatrix}$$

For each point  $p$ , all map edges  $m$  are selected that are within some radius  $R$  of  $p$ .

$$M_p = \{m \mid d(b, p) \leq R \wedge d(e, p) \leq R\}$$

For these sets of edges the moments of the edge vector components are calculated. In the summation, the length of the edge vectors is used as a weight. In this way, the moments do not depend on the maximum distance between the map points used for the densification of the map points.

$$N_p = \begin{pmatrix} \sum_{m \in M_p} \|m\| x_n^2 & \sum_{m \in M_p} \|m\| x_n y_n \\ \sum_{m \in M_p} \|m\| x_n y_n & \sum_{m \in M_p} \|m\| y_n^2 \end{pmatrix}$$

The eigenvalues of this matrix indicate whether the map edges show dominant edge directions. Figure 5 shows the colour coded map points and laser points of the road parts. Points shown in blue are points with an eigenvalue ratio below 3. These points are located near corners in the street pattern. For these points, the height has been calculated with the unconstrained 2<sup>nd</sup> order polynomial fit as used in figure 4. Points shown in green have an eigenvalue ratio of at least 3. These points are located on straight road segments. For these points a polynomial fit has been applied that only allows a slope and a curvature in the direction of the eigenvector belonging to the largest eigenvalue (i.e. the main road direction).

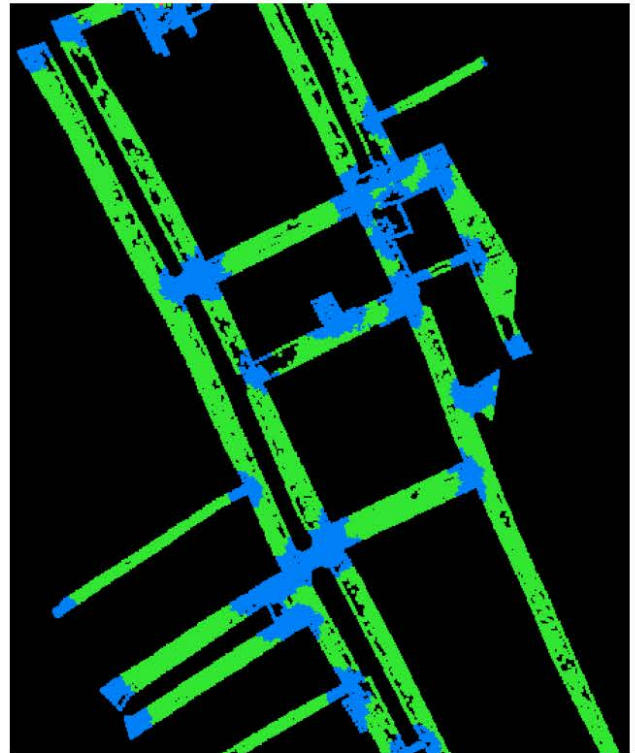


Figure 5: Classification of points based on the isotropy of the edge directions within a radius of 10 m. In green (light grey), positions near street corners, in blue (dark grey) positions on straight street segments. The black holes in the street surfaces are areas without reflected laser pulses.

Formally, the unconstrained polynomial fit is performed with the observation equation

$$Z(X, Y) = a_{00} + a_{10}X + a_{01}Y + a_{20}X^2 + a_{11}XY + a_{02}Y^2$$

set up for all points within some radius of the point for which the height needs to be estimated. The slope and the curvature in the direction perpendicular to the road axis is disabled by constraining the estimation of the coefficients with the equations

$$\begin{pmatrix} \cos \alpha & \sin \alpha & 0 & 0 & 0 \\ 0 & 0 & -2 \sin \alpha \cos \alpha & \cos^2 \alpha - \sin^2 \alpha & 2 \sin \alpha \cos \alpha \\ 0 & 0 & \cos^2 \alpha & \sin \alpha \cos \alpha & \sin^2 \alpha \end{pmatrix} \begin{pmatrix} a_{10} \\ a_{01} \\ a_{20} \\ a_{11} \\ a_{02} \end{pmatrix} = \mathbf{0}$$

in which  $\alpha$  is the normal direction to the road axis represented by  $X \cos \alpha + Y \sin \alpha = d$ . These equations constrain the across road slope, torsion and across road curvature, respectively to zero.

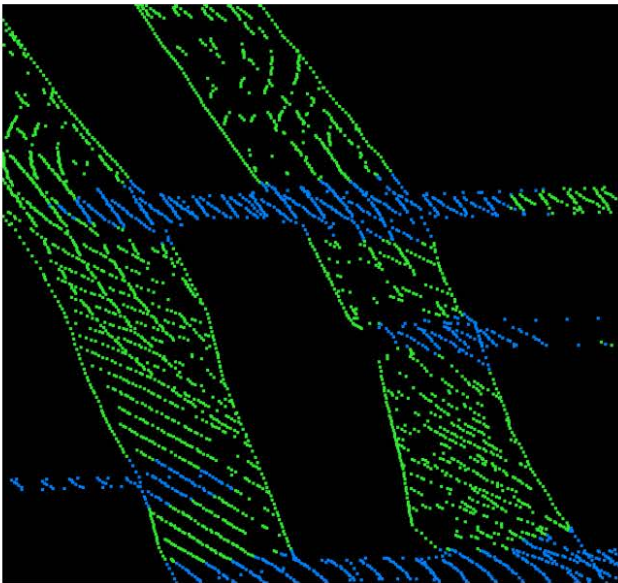


Figure 6: Classification of points for the example used in figures 3, 4 and 7.

The results are shown in figures 6 and 7. Figure 6 shows the point classification from about the same viewpoint as the other figures of the reconstructed road surface. Figure 7 shows the reconstructed surface using the constrained estimation for the points that are shown in green in figure 6. Compared to the results of the unconstrained polynomial fitting of figure 4, the

estimation of the height of the road sides is clearly improved and now much more realistic. The estimation of the curvatures of the bridges across the canals is not affected by the constraints.

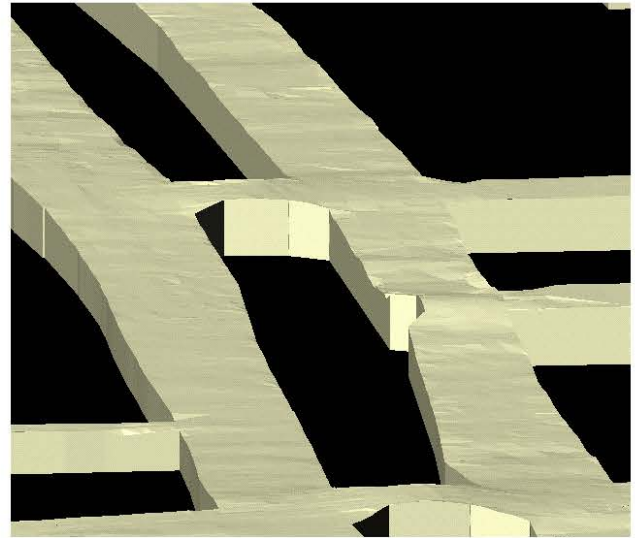


Figure 7: Road surface estimated by the constrained 2<sup>nd</sup> order polynomial fitting to near laser points.

The results can be further analysed by comparing the heights assigned to the nodes of the map edges by the different methods. Figure 8 shows the heights assigned to a roadside adjacent to buildings. Note that the scales along both axes differ by a very large factor (25)! The heights obtained from the nearest laser points (black profile) show very strong local variations. These are caused by reflections of the laser pulses on small fences, poles and other objects standing in front of the buildings. Some points are quite low and might indicate errors due to corner reflection. The heights estimated from the 2<sup>nd</sup> order polynomial fit still show considerable fluctuations on this road segment (which is quite flat in reality). In particular in the central segment the heights seem to be overestimated due to incorrectly determined across-road curvature. The profile obtained with the constrained fitting approach is relatively smooth. Although the height variations may still be a little affected by reflections of laser pulses on low non-terrain objects, the estimated heights will generally be within 5-10 cm of the correct street level.

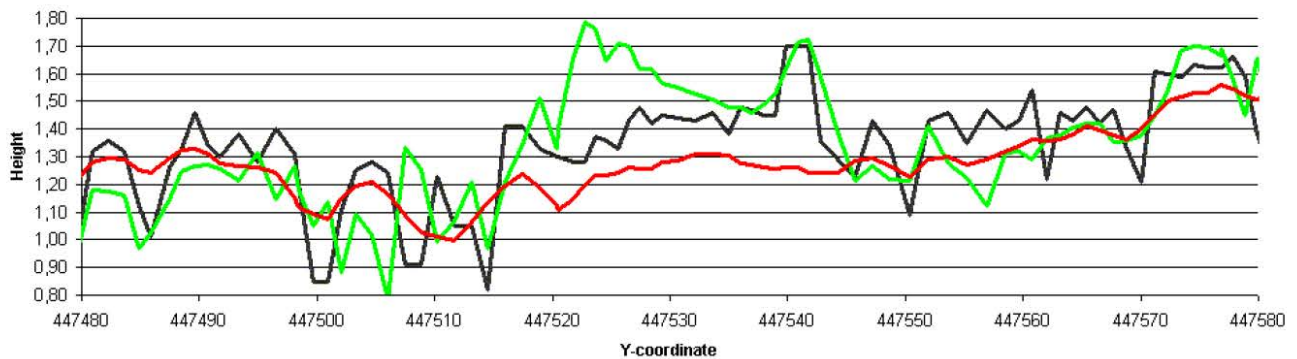


Figure 8: Roadside profiles reconstructed by three different methods: height of nearest laser point (black), 2<sup>nd</sup> order polynomial fit (green) and constrained 2<sup>nd</sup> order polynomial fit (red).

### 3. DETECTION OF TREES

Trees in the streets have an important impact on how a city is perceived. Adding trees to a city model improves the impression one can obtain. Brenner and Haala (1998) used colour infrared imagery to extract the location and planimetric extent of trees and added tree models to their city model. For the determination of the tree locations they used the node points of the skeletons of vegetation areas. These vegetation areas were obtained by an ISODATA classification.

With the increasing pulse rates of laser scanners the point densities increased to a level that even smaller trees might now be extracted from laser data. This was verified by first selecting all points within the road and water parcels that are 5 or more meters above the ground level. Due to small inaccuracies, map generalisations and objects attached to buildings this data contains many points that do not belong to trees. The selected data was further reduced by removing all points within some distance of buildings. In this dataset the locations of the trees were detected by determining the local maxima of the laser points. A window size of 3 meters was found to yield to best results.

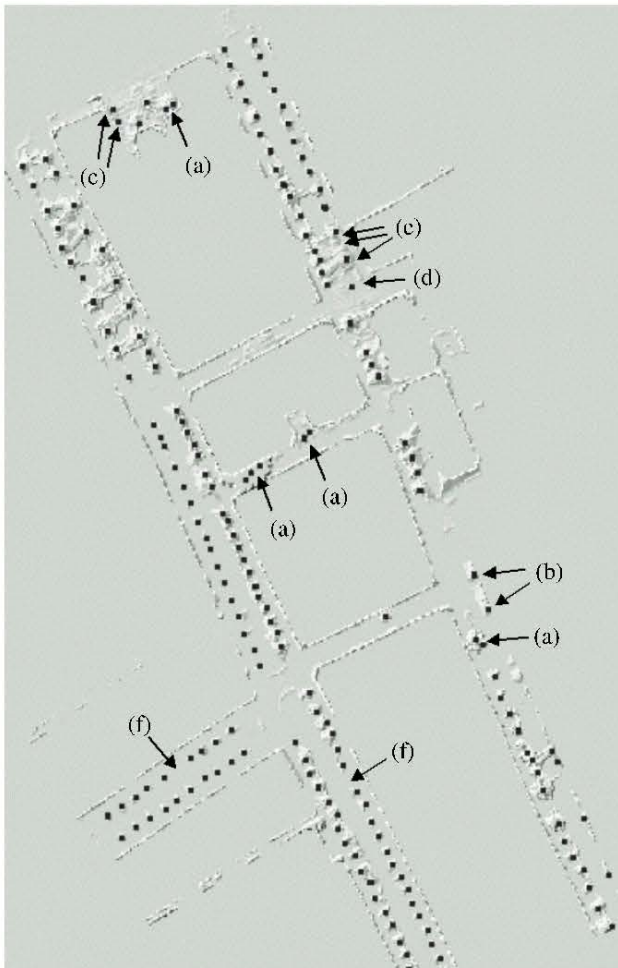


Figure 9: Detection of tree locations with indicated errors. Multiple locations identified for the same tree (a). Small buildings (b), sun-shades (c) or street light (d) detected as tree. Small trees near larger trees (e) and trees without reflections in the laser data (f) are missed.

The results are shown in figure 9. The background in this figure is a shaded relief image of the heights of all points that were initially selected. The edges of the buildings are clearly recognisable in this image. The extraction of the tree locations was verified on the spot. Of the 182 trees in the processed streets, 177 trees were detected, corresponding to a detection rate of 97%. Of the five small trees that were missed, three were located near large trees and therefore we not found as local maxima. Two small trees did not at all appear in the laser data. Due to the point distance of 2 meters in scanline direction and the fact that last pulse data was recorded, no pulses reflected from these trees.

Nine trees were incorrectly identified, corresponding to a false alarm rate of 5%. Four large trees were counted double, as two local maxima were detected in the crowns of these trees. Two small buildings were classified as tree. These buildings were not marked as building parcels in the cadastral map. Furthermore, two large sunshades on a restaurant pavement and one large street light were identified as trees.

To model the shape of the tree crowns, all laser points were assigned to an assumed tree location (i.e. local maximum). For each point that tree was selected for which the slope of the line connecting the point and the local maximum of the tree was maximal. Attempts to model the tree crowns showed that reasonable shapes could be extracted for the larger trees with a few hundred points on the crown. Many trees crowns, however, were only represented by ten or less points. This resulted in unrealistic crown shapes. In the produced city models, the trees were therefore represented by a fixed shape model with the width as a function of the height of the local maximum (figures 11 and 12). In figure 12 it can be seen that some of the larger trees models have been placed in the canal. Because of the proximity of the buildings, the trees tend to grow more into the direction of the canal. Consequently, the locations of the local maxima do not always correspond to the location of the tree trunk. For a realistic modelling, such tree locations, of course, would need to be corrected. This can be done by making use of the cadastral map. Trees located in the water areas can be moved to the nearest location in a street parcel.

### 4. MODELLING CANALS AND BUILDINGS

To complete an initial 3D city model, the canals and buildings were modelled by polyhedral objects with a horizontal top surface. The water level in the canals was determined by examining the histogram of the heights of all points in the water parcels (figure 10).

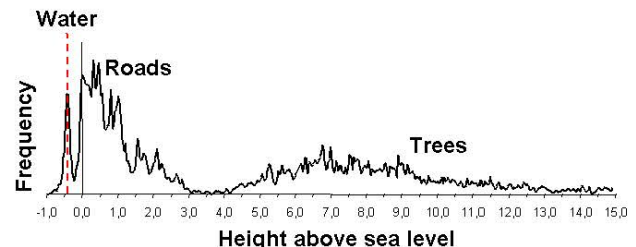


Figure 10: Histogram of all points in the water objects. Only a very small percentage of the laser pulses is actually reflected by the water surface.

Striking is the relatively low percentage on points that reflected on the water surface. Many reflections are caused by tree

branches over the water surface, by road parts near the edges of the water areas and by several boats in the canals. Despite the small percentage of points that actually reflect from the water surface, the water level can easily be extracted from the histogram. The determined water level of 0.4 m below sea level indeed corresponds to the actual water height.

The roof landscape was not modelled in this project. To get a rough impression for each building parcel, the height of a flat roof was set to the 90% value of the height in the histogram of the points within the parcel bounds. This value was chosen to avoid extremely high building models caused by a few outliers in the height data.

Two views of the completed model are shown in figures 11 and 12.

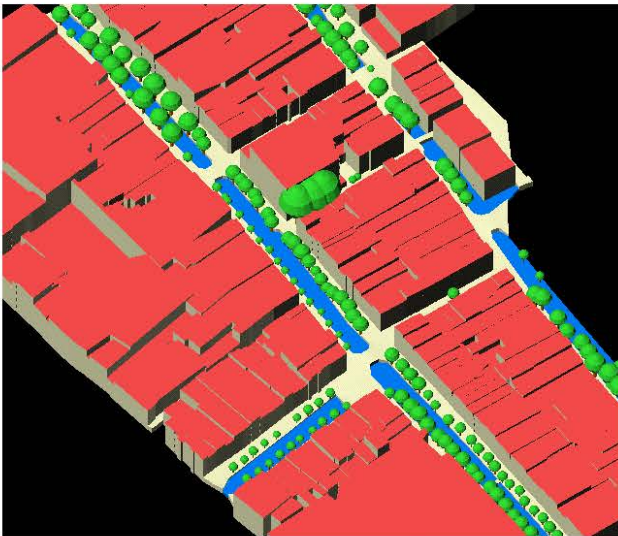


Figure 11: Bird's eye view of the 3D model.

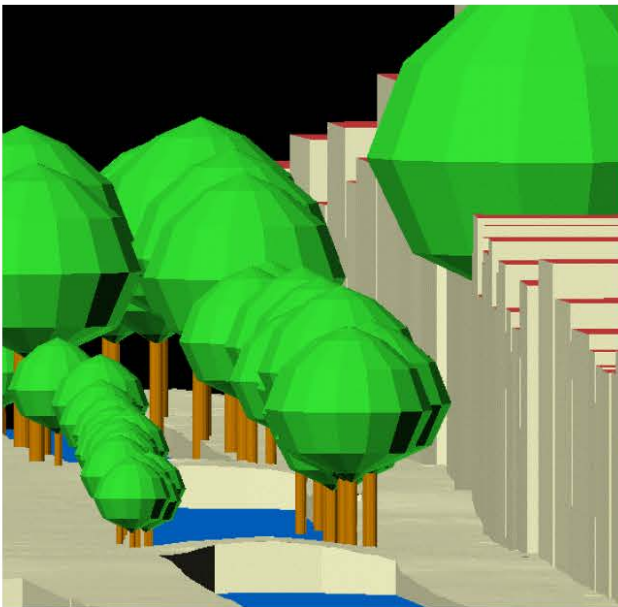


Figure 12: Street level view of the 3D model.

## 5. CONCLUSIONS

City models that are to be used for city planning and tourism applications require the modelling and extraction of street surfaces and trees. The availability of cadastral maps is

considered of large value for the extraction of these objects from airborne laser data. To both model the street surface and extract the location of trees, both first and last pulse data should be recorded. Flights should preferably be conducted in the leafless season. The data used in this project was flown in August. Despite the last pulse mode, large road surface parts are complete occluded by larger trees with dense foliage.

For the extraction of the crown shape of the trees, a higher point density is needed than the used two meter point spacing in scanline direction. A higher point density and the usage of first pulse data, will of course also improve the detection rates of trees in the laser data. By analysing the structure of the point clouds that are assigned to an assumed tree location, the higher point density may also allow an automatic detection of false alarms caused by objects like small buildings and sunshades. Due to the small number of points per object, such an analysis was not possible in this project.

## ACKNOWLEDGEMENTS

The laser altimetry data used in this research was acquired by Aerodata Int. Surveys using the TopoSys I scanner and processed by TopoSys GmbH. Kadata B.V. provided the cadastral data. The author would like to thank all companies for their contributions to this research project.

## REFERENCES

- Baltsavias, E.P. (1999) Airborne laser scanning: existing systems and firms and other resources. *ISPRS Journal of Photogrammetry and Remote Sensing* 54 (2-3), 164-198.
- Brenner, C., N. Haala (1998) Fast production of virtual reality city models. *International Archives of Photogrammetry and Remote Sensing*, vol. 32, part 4, pp. 77-84.
- Haala, N., C. Brenner, K.-H. Anders (1998) 3D urban GIS from laser altimeter and 2D map data, *International Archives of Photogrammetry and Remote Sensing*, vol. 32, part 3/1, pp. 339-346.
- Rottensteiner, F., C. Briese (2002) A New Method for Building Extraction in Urban Areas from High-Resolution LIDAR Data, *International Archives of Photogrammetry and Remote Sensing*, vol. 34, part 3A, pp. 295-301.
- Sithole, G., G. Vosselman (2003) Automatic structure detection in a point cloud of an urban landscape. Accepted for presentation at the 2<sup>nd</sup> GRSS/ISPRS Joint Workshop on Remote Sensing and Data Fusion over Urban Areas, URBAN2003, Berlin, May 22 – 23.
- Vosselman, G. (1999) Building Reconstruction Using Planar Faces in Very High Density Height Data. *International Archives of Photogrammetry and Remote Sensing*, vol. 32/3-2W5, Munich, Germany, pp. 87-92.
- Vosselman, G. (2000) Slope based filtering of laser altimetry data. *International Archives of Photogrammetry and Remote Sensing*, vol. 33, part B3, pp. 935-942.